This is the accepted manuscript made available via CHORUS. The article has been published as:

Fine structure in the odd-odd proton emitter math xmlns="http://www.w3.org/1998/Math/MathML">mmultiscripts>mi>Tm/mi>mprescripts>/mprescripts>none>/none>mn>144/mn>/mmultiscripts>/math>

Pooja Siwach, P. Arumugam, S. Modi, L. S. Ferreira, and E. Maglione

Phys. Rev. C **105**, L031302 — Published 17 March 2022

DOI: 10.1103/PhysRevC.105.L031302

Fine structure in odd–odd proton emitter ^{144}Tm

Pooja Siwach,[1,2] P. Arumugam,[1,*] S. Modi,[3] L. S. Ferreira,[4] and E. Maglione[4]

[1]*Department of Physics, Indian Institute of Technology Roorkee, Roorkee-247667, Uttarakhand, India*
[2]*Department of Physics, University of Wisconsin, Madison, Wisconsin 53706, USA*
[3]*Department of Physics, BIT Sindri, Dhanbad, Jharkhand-828121, India*
[4]*Centro de Física e Engenharia de Materiais Avançados CeFEMA, and Instituto Superior Técnico, Universidade de Lisboa, Avenida Rovisco Pais, P1049-001 Lisbon, Portugal*

(Dated: March 1, 2022)

Axial symmetry breaking in ^{144}Tm is probed by examining its proton emission fine structure. The ground state spin and parity in ^{144}Tm and daughter ^{143}Er are assigned unambiguously based on the corroboration of our calculations with the present data. We establish the first microscopic description of fine structure in odd–odd proton emitters, which is capable of resolving ambiguities present in the assignments of transitions in such nuclei.

Owing to energy requirements, most of the proton emitters populate only the ground states of the daughter nuclei. However, when other appropriate states are available at low excitation energy, significant branching can occur to these states leading to fine structure in the emission spectrum. Since the spacing between excited states depends mainly on the deformation, the proton emission fine structure is an excellent tool to probe the nuclear structure properties beyond drip-line. Among around thirty known proton emitters in the region $50 \leq Z \leq 82$, fine structure is exhibited by three odd-A (^{131}Eu [1], ^{141}Ho [2], ^{145}Tm [3]) and two odd–odd (^{144,146}Tm [4–6]) nuclei only. In odd-A proton emitters this phenomenon is well understood due to robust theoretical approaches [7–9]. However, a microscopic description of fine structure in ^{144,146}Tm is still missing.

The investigation of fine structure in proton emission provides a reliable way to identify the ground state spin and parity, along with the deformation of nuclei beyond the proton drip-line. For instance, in ^{141}Ho [9] and ^{145}Tm [8], fine structure studies are found to be very accurate in ascertaining the triaxial deformation. Such studies are more critical in odd–odd nuclei where the information on the level scheme of exotic daughter odd-A nuclei themselves are scarce and complex. Furthermore, in the parent odd–odd nucleus, various possible angular momentum couplings lead to numerous levels close to each other and many of them may have a similar configuration. Consequently, several levels can reproduce the measured half-life in odd–odd nuclei. One way to rule out these possibilities is to look for the level with the lowest energy and favored by the GM-splitting [10] and Newby shift [11]. This way of proceeding has been proved reliable in ^{108}I [12]. Another more reliable way to resolve these ambiguities is the investigation of fine structure, if available. Though many levels can reproduce the measured half-life, only a few can agree with the measured branching ratio and partial half-lives because of the additional constraint through the excited state in the daughter [7]. Moreover, the calculated branching ratios are almost insensitive to various parameters of the model [8].

For the above reasons, it is interesting to study the fine structure in the proton emission spectra of ^{144}Tm. In the experimental study [4], two proton groups with different energy but comparable half-life were observed, suggesting that they might originate from the same state. The spin-parity assignment for these transitions, guided by the cases of ^{145,146}Tm, is still unclear. Furthermore, the assignment for transitions in ^{146}Tm [5, 6] itself is tentative and based on the modified particle-vibrator model [13] in which the valence neutron is treated as a mere spectator. Also, the single-particles are treated in a spherical potential, whereas the neighbouring nuclei ^{145,147}Tm [8, 14, 15] are well established to be highly triaxial. Moreover, the residual pairing interaction is not considered properly, which is very crucial in proton emission studies [16]. Also the *np* interaction is missing, which is very important to the assignment of the lowest state in energy. The absence of a robust theoretical approach for triaxial odd–odd nuclei has led to ambiguities resulting in different assignments of these transitions [5, 6, 17]. It hence has hampered achieving the goal of such a tedious task performed to measure these transitions. In this work, we present the first microscopic description of fine structure in triaxial odd–odd nuclei by extending the nonadiabatic quasiparticle approach [12, 18, 19]. One of the major advantages of this approach is that the matrix elements of the coupled system explicitly carry the rotor's matrix element in the lab frame [18]. This provides the opportunity to utilize the rotor's experimental data, which in turn reduces the dependence on several adjustable parameters. Most of the details of our formalism are reported elsewhere [12, 18, 19] and hence a concise description relevant to the calculation of fine structure is presented in the next section.

In the nonadiabatic quasiparticle approach, we treat a triaxial odd–odd nucleus as a composite system of two quasiparticles (corresponding to the valence proton

*Electronic address: Corresponding Author - arumugam@ph.iitr.ac.in

and the valence neutron) weakly coupled to an even–even core. The total Hamiltonian for such a system comprises the Hamiltonian for dynamics of core, single-particle (proton and neutron) motion, the residual pairing interaction, and the residual neutron–proton (np) interaction. The triaxial Woods–Saxon potential is considered for describing the single-particle motion. The residual pairing interaction is treated within the BCS approach. The residual np interaction is considered in two reliable forms, namely the constant potential form and the zero-range interaction (δ interaction). The detailed expressions for all these terms leading to the matrix elements of the total Hamiltonian are given in Ref. [18].

The overlap of the wave function of an odd–odd nucleus (parent) with that of final state wave function (a tensorial product of daughter and proton wave function at asymptotic limit) provides the decay width. The partial decay width of proton emission can be expressed as [12]

$$\Gamma^{II_d}_{l_pj_p} = \frac{\hbar^2 k}{\mu}\left(\frac{2I_d+1}{2I+1}\right) \times \Big| \sum_{\Omega_p j_n \Omega_n K_d \Omega K} a^{I_d}_{j_n\Omega_n K_d} c^{I}_{\Omega_p\Omega_n\Omega K}\Big(\langle I_d K_d j_p \Omega_p | IK\rangle + (-1)^{I_d-K_d}\langle I_d - K_d j_p \Omega_p | IK\rangle\Big) u_{\Omega_p} N^{\Omega_p}_{l_pj_p}\Big|^2. \quad (1)$$

Here a's and c's are the mixing coefficients in parent and daughter wave functions, respectively. The terms in the angular braces represent the Clebsch–Gordan coefficients. The quantities $l_{p(n)}, j_{p(n)}$ and $\Omega_{p(n)}$ are the quantum numbers of proton (neutron) orbital with the usual meaning. I and I_d denote the total spin of parent and daughter nucleus, respectively, and their projection on 3-axis are denoted by K and K_d. The square of u_p signifies the probability of proton level to be empty in the parent nucleus. k is the momentum of emitted proton and μ is the reduced mass of the system. The quantity $N^{\Omega_p}_{l_pj_p}$ is the normalisation constant [20] given by $\phi^{\Omega_p}_{l_pj_p}(R)/[G_{l_p}(kR)+\iota F_{l_p}(kR)]$ where F and G are the regular and irregular Coulomb wave functions, respectively, and ϕ is the radial part of proton wave function. The total decay width can be obtained by summing over all the states as follows

$$\Gamma^{II_d} = \sum_{j_p=|I-I_d|}^{I+I_d} \Gamma^{II_d}_{l_pj_p}. \quad (2)$$

The corresponding half-life is given by

$$T_{1/2} = \frac{\hbar \ln 2}{\Gamma^{II_d}}. \quad (3)$$

The branching ratio for the transition to the excited state of a daughter can be obtained as $\Gamma^{II'_d}/(\Gamma^{II_d}+\Gamma^{II'_d})$, where I'_d denotes the spin of the excited state of daughter nucleus.

The decay scheme of a proton emitter substantially depends on the properties of its daughter nucleus. Therefore, we begin with the investigation of the properties of ^{143}Er which is the daughter of ^{144}Tm after proton emission. Due to the unavailability of the data for ^{142}Er (core of ^{143}Er and ^{144}Tm), the nearest even–even nucleus ^{142}Dy is considered as a core, similarly to earlier studies [8, 15]. For the positive parity states, we couple the neutron levels from 13$^{\text{th}}$ to 22$^{\text{nd}}$ (counted from bottom) which include levels with parentage $1g_{9/2}, 1g_{7/2}, 2d_{5/2}, 3s_{1/2}$ and $2d_{3/2}$. The negative parity levels from 14$^{\text{th}}$ to 22$^{\text{nd}}$ originating from $1h_{11/2}, 2f_{7/2}$ and $1h_{9/2}$ orbitals are considered for the corresponding rotational states. The rotational energies obtained for positive and negative parity states are given in FIG. 1. Since the states are obtained considering the core (predominantly of rotational nature) coupled to quasiparticles, we mention them commonly as rotational states that may or may not belong to the same rotational band. The values of β_2 and β_4 are chosen to vary around the ones suggested by macroscopic–microscopic calculations [21] and considered in several other studies [8, 14]. In the axially deformed ($\gamma = 0°$) case, the $7/2^+$ state is the lowest in energy among positive parity states in the probable deformation region. This is valid for $\gamma \lesssim 30°$. Beyond $\gamma \approx 30°$, the levels $1/2^+$ and $3/2^+$ come down due to the crossing of $3s_{1/2}$ and $2d_{3/2}$ quasiparticle levels.

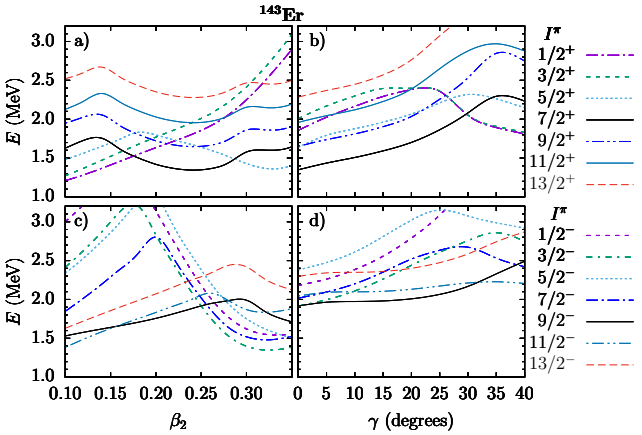


FIG. 1: The positive [negative] parity rotational states of ^{143}Er a) [c)] as a function of β_2 and b) [d)] as a function of γ at $\beta_2 = 0.25$ and $\beta_4 = -0.074$.

Among the negative parity states, the $9/2^-$ is the lowest in energy for $0.15 \lesssim \beta_2 \lesssim 0.25$ and $\gamma = 0°$. Beyond $\beta_2 \approx 0.25$, many lower spin levels cross due to crossing of $2f_{7/2}$ quasiparticle levels. With an increase in γ, the $9/2^-$ is consistently lowest in energy followed by the $11/2^-$ in the probable deformation region. It is well established in many studies [8, 14, 15] that the ground state proton emission in neighbouring isotopes ^{145,147}Tm occurs from a negative parity state. Therefore, we consider the negative parity proton levels from 14$^{\text{th}}$ to 19$^{\text{th}}$ which

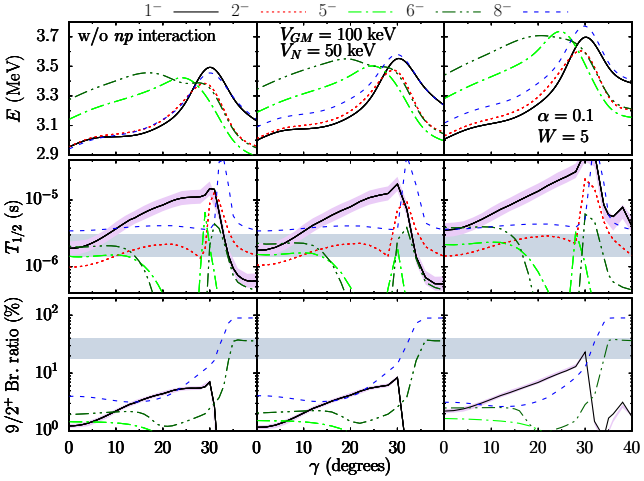


FIG. 2: Rotational energies (top panels), total proton emission half-lives (middle panels) and branching ratios (bottom panels) for ^{144}Tm. Results without *np* interaction, with *np* interaction in constant potential form and zero-range form are given in first, second and third column, respectively. The experimental data taken from Refs. [4, 22] are shown in grey. The width in violet represents the uncertainty in the results due to the experimental uncertainty in the Q_p values.

include orbitals of $1h_{11/2}$ and $2f_{7/2}$ origin. We examine the transition to both negative and positive levels of daughter nucleus ^{143}Er. For the negative parity levels in ^{144}Tm, the calculated rotational energies and the total half-lives along with the branching ratios for the first probable excited state ($9/2^+$) are given in FIG. 2. As stated earlier, among the positive parity levels in ^{143}Er, the $7/2^+$ state is the lowest in energy in the probable deformation region followed by the $9/2^+$. Note that the $5/2^+$ is also close to the $9/2^+$ but the transition to it is not found consistent with the measured branching ratio due to its different configuration. In the absence of the residual *np* interaction, we infer from the rotational energies that the $1^-, 2^-$, and 8^- states are the lowest and almost degenerate in region $\gamma \lesssim 25°$. Beyond this γ value, the 5^- turns out to be the lowest in energy with the 2^- and 6^- close by. Including the *np* interaction, the degeneracy in the 1^- and 8^- is lifted pushing the 8^- up in energy due to its singlet nature in consistency with the GM rule [10]. The calculated half-lives for the considered states assuming transitions to the $7/2^+$ (ground) and $9/2^+$ (first excited) states of the daughter agree well at $\gamma = 0°$. However, the measured branching ratio is not reproduced for any of these states. The branching ratio for the 8^- state is in range with the measured one for $\gamma \approx 30°$ where the corresponding half-life does not agree with the measured one. A similar behavior is observed for the 1^- and 6^- states. The branching ratios for other states are found to be out of the range, and hence are not considered here.

The effect of the residual *np* interaction is studied in two different form, a constant potential and a zero-range interaction. Due to the scarcity of the data in the considered exotic region, the values for the strength parameters V_{GM}, V_N, α, and W of the *np* interaction cannot be estimated, and hence they are chosen as the standard ones to analyse their qualitative effect only. It can be observed from the results given in FIG. 3, that the residual *np* interaction does not affect noticeably the half-lives and branching ratios. Since for $\gamma \gtrsim 30°$, the $1/2^+$ and $3/2^+$ states of the daughter are lower in energy, we calculated the half-lives and branching ratios corresponding to these states also. The results are found to be not in agreement with the experimental data in the probable deformation region, and hence are not presented here. Therefore, the transition to the positive parity states of daughter nucleus is very unlikely. A better understanding can be obtained from the analysis of partial half-lives as explained later.

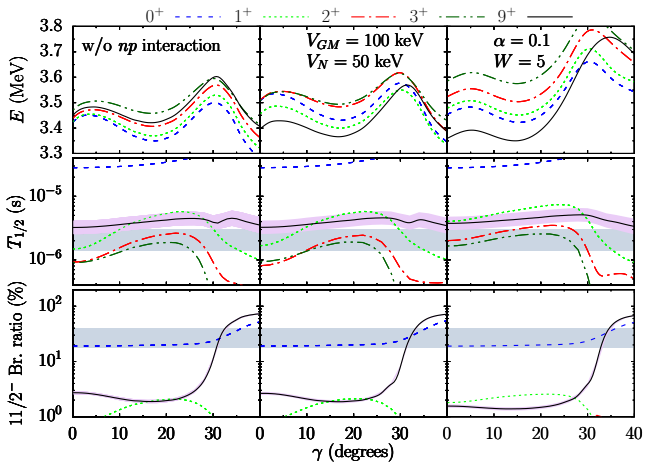


FIG. 3: Same as FIG. 2 but for positive parity states.

We proceed to analyse the case of transition from positive parity states of the parent nucleus to the negative parity $9/2^-$ (ground) and $11/2^-$ (first excited) states of the daughter nucleus. The results for this case are given in FIG. 3. When the residual *np* interaction is not incorporated, the rotational energy of the 0^+ state is minimum, however, the other states $(1^+, 2^+)$ are also very close to it. Though the branching ratio is very well reproduced for all considered values of γ, the proton emission half-life corresponding to the 0^+ state is out of range and does not reproduce the measured one. Therefore, the 9^+ is the only possible state for which measured half-life and branching ratio are very well reproduced at $\gamma \approx 30°$. This assignment is also supported (because of its triplet nature) by the *np* interaction.

In the experimental study of Ref. [4], the proton emitting state was suggested to be either 10^+ or 5^-. However, in our calculations the 10^+ is found to be very high in energy and also the measured values are not reproduced. The 5^- state also cannot reproduce the branching ratio. These disagreements can be understood in terms

of the shortcomings of the theoretical model [13] used in Ref. [4]. Apart from the absence of residual pairing and *np* interactions, as mentioned above, in this model, the wave function is truncated to 1-phonon basis states. This assumption will work if the coupling between 0 and 1-phonon states is small, as it should be in a vibrational model. However, the wave function has about 50% contribution from 0 and 1-phonon states [4, 6, 23] both. Including two-phonon basis states would further decrease the 0-phonon part, as can be learnt from the study of Ref. [24]. So, it seems that the coupling strength used is too large, which will increase the decay to the excited state with respect to the ground state. Therefore the assignment of the 10^+ is very questionable.

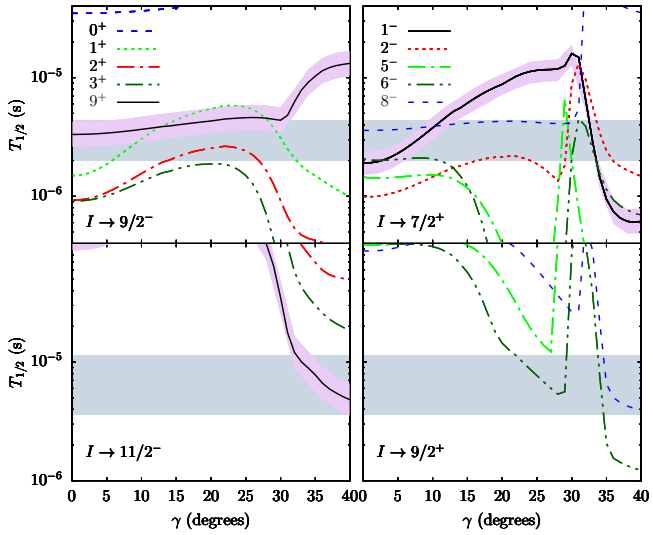


FIG. 4: Partial proton emission half-lives corresponding to transitions to ground (top) and first excited (bottom) states of the daughter nucleus from positive (left) and negative parity (right) states of ^{144}Tm.

To further strengthen our arguments, the partial half-lives for the transitions to ground and first excited states are given in FIG. 4. In the case of positive parity states, for the 9^+, the half-lives for both transitions reproduce well the measured data at $\gamma \approx 30°$. However, the partial half-lives for none of the negative parity states simultaneously agree with the measured values. For instance, the half-life for the 8^- state reproduces the transition to the $7/2^+$ state in the region $\gamma \lesssim 30°$, but does not agree in case of transition to the $9/2^+$. Similar arguments are true for other cases. Therefore, we can unambiguously assign the spin and parity to the ground state of ^{144}Tm as 9^+. Furthermore, the ground and first excited state spin and parity in ^{143}Er are assigned to be $9/2^-$ and $11/2^-$, respectively. The assignment of $9/2^-$ is in agreement with the one suggested in Ref. [25].

One of the motives to study proton emission is to investigate the organisation of single-particle levels beyond the drip-line. The contributions of single-particle levels in the ground state along with the probability of $K[= K_R + \Omega_p \pm \Omega_n]$ (projection of I on 3-axis) distribution are given in FIG. 5. In the case of the 1^- and 8^- states, the $\{\pi h^{5th}_{11/2} \otimes \nu g^{4th}_{7/2}\}$ is the dominant configuration, and the probabilities for $K = 1$ ($p|K| \approx 86\%$) and 8 ($p|K| \approx 46\%$) are maximum, respectively. Therefore, we can approximately infer the nature (singlet or triplet) of final states by analyzing the resulting total spin projection from the single-particle ones (Σ_p, Σ_n). The asymptotic quantum numbers [26] of $h^{5th}_{11/2}$ and $g^{4th}_{7/2}$ levels are [514]9/2 ($\Sigma = 1/2$) and [404]7/2 ($\Sigma = -1/2$), respectively. Noticing the dominance of $K_R = 0$ in the lower lying states, $K \approx \Omega_p \pm \Omega_n$ points that 1^- and 8^- states have the strongest contribution from the $\Omega_p - \Omega_n$ $(\Sigma_p - \Sigma_n)$ and $\Omega_p + \Omega_n$ $(\Sigma_p + \Sigma_n)$, respectively. Therefore, we can infer from these asymptotic quantum numbers that the 1^- and 8^- are predominantly triplet ($\Sigma = 1$) and singlet ($\Sigma = 0$) states, respectively. This observation further discards the 8^- as a probable ground state following the GM rule [10] which favors the triplet state (1^-). The triplet state being energetically favored due to *np* interaction is also evident from FIG. 2. The other considered negative parity levels have $\{\pi h^{4th}_{11/2} \otimes \nu s^{1st}_{1/2}\}$ as the dominant configuration, and a strong mixing of many K's. For positive parity states, the $\{\pi h^{5th}_{11/2} \otimes \nu h^{5th}_{11/2}\}$ is the dominant configuration and the probability of $K = I$ is maximum, and for the 9^+ state it is $p|K| \approx 50\%$. Following the same analysis as for the negative parity states, the 0^+ and 9^+ can be identified as singlet and triplet states, respectively, supporting the 9^+ as the ground state. For the considered levels, the residual *np* interaction does not change the configuration significantly. This happens due to the large deformation where the mixing of levels is weak as it can be noticed in FIG. 5. Therefore, we do not observe any significant change in the half-lives and the branching ratios in the presence of *np* interaction.

In line with Ref. [21], one might suspect the role of γ-softness, whereas we have performed the calculations at fixed β and γ values. As pointed out in Ref. [18], our formalism can be extended to study the role of γ-softness by considering a superposition of states with different γ's. However, we notice from Figures 2, 3, and 4 that the branching ratio and decay width (inversely proportional to half-life) corresponding to the excited state for $\gamma \lesssim 30°$ are negligible. Therefore, considering a superposition of the states with various γ's will reduce the contribution from higher γ and will lead to a smaller decay width (large $T_{1/2}$) and a branching ratio that does not reproduce the experimental data. Hence, components leading to a large partial decay width only should contribute to the ground state wave function. This is fulfilled only by the states with a large γ in a narrow region around 30°.

Analyzing the transitions to both positive and negative parity states of the daughter, we arrive at the conclusion that the transition to the positive parity states of the daughter is not possible. Though the half-lives corresponding to several states of the parent nucleus agree well with the measured data, the branching ratios are

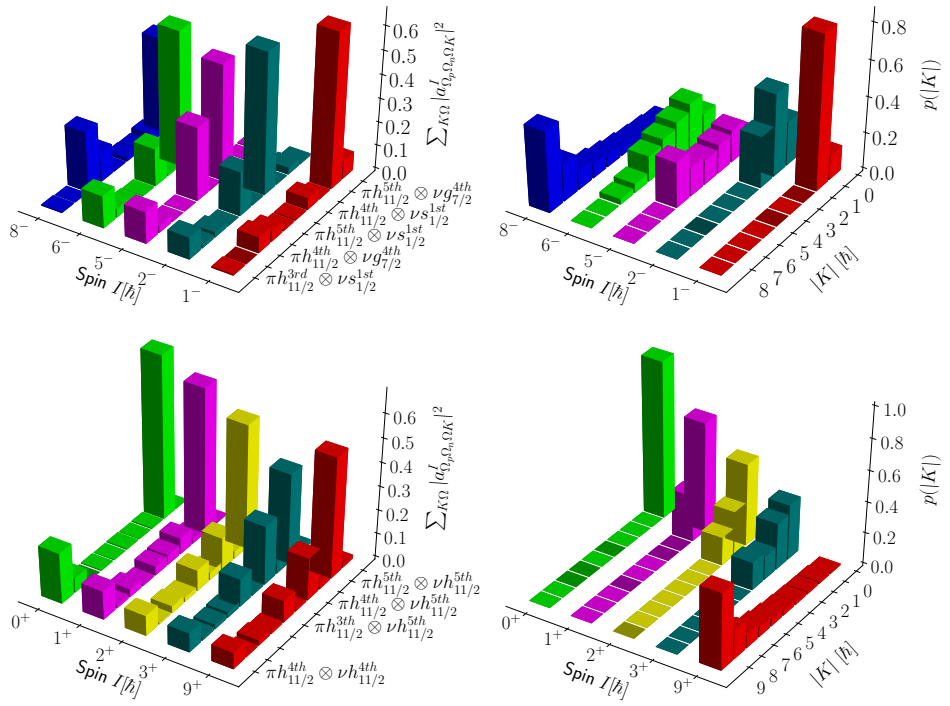


FIG. 5: The contribution of single-particle configurations (left) and the probability of K distribution (right) in the negative (top) and positive (bottom) parity states of ^{144}Tm. The dominant single-particle configurations are labeled.

found to be helpful in ruling out the possibilities for those states. Furthermore, among the positive parity states of the parent, the 9^+ is the only possible state reproducing all the measured properties *viz.*, the total half-life, partial half-lives and the branching ratios, simultaneously at $\gamma \approx 30°$. The residual *np* interaction further supports this assignment (9^+) due to its triplet nature.

The triaxial deformation proposed in this work is in agreement with the one in nearby nuclei [8, 14, 15]. However, the disagreement with Ref. [21], where ^{144}Tm is suggested to be axially deformed, lies in the fact that the microscopic-macroscopic calculations involve several parameters to be tuned, which makes them unreliable in drip-line nuclei due to lack of data. Because of the crucial role of the residual *np* interaction, these difficulties enhance in the case of odd–odd nuclei. Such disagreements for several other proton emitting nuclei [8, 9, 12, 14, 15, 27, 28] further strengthen the necessity of novel tools to probe the nuclear structural properties of drip-line nuclei. It is clear that the microscopic-macroscopic calculations, rotation-particle coupling calculations, etc, which focus only on the structure part of the drip-line nuclei leads to ambiguities. A unified description of structure and decay is required to ascertain properties of such exotic nuclei as exemplified in this work.

The fine structure in proton emission from ^{144}Tm is studied within the nonadiabatic quasiparticle approach. This is the first microscopic study of fine structure in proton emission from odd–odd nuclei. The ^{144}Tm is found to be highly triaxial with $\gamma \approx 30°$. Corroboration of our results with the present data allows us to unambiguously assign the ground state spin and parity of ^{144}Tm to be 9^+. Furthermore, the ground and first excited state spin and parities in ^{143}Er are assigned to be $9/2^-$ and $11/2^-$, respectively. With the present investigation, we settle the uncertainties pointed out in earlier work and provide a robust explanation of the level scheme. Similar calculations for other odd–odd nuclei like ^{146}Tm would be interesting where the fine structure in proton emission is observed but no clear assignment is available. The nuclei in proton drip-line region continue to be puzzling and surprising [29] which demands novel techniques and approaches. Further studies exploring the proton emission and gamma spectrum simultaneously can provide a robust way to understand the nuclear properties in this exotic region.

Acknowledgments

This work was supported in part by the U.S. Department of Energy, Office of Science, Office of High Energy Physics, under Award No. DE-SC0019465.

[1] A. A. Sonzogni, C. N. Davids, P. J. Woods, D. Seweryniak, M. P. Carpenter, J. J. Ressler, J. Schwartz, J. Uusitalo, and W. B. Walters, Phys. Rev. Lett. **83**, 1116 (1999), URL http://link.aps.org/doi/10.1103/PhysRevLett.83.1116.

[2] M. Karny, K. Rykaczewski, R. Grzywacz, J. Batchelder, C. Bingham, C. Goodin, C. Gross, J. Hamilton, A. Korgul, W. Królas, et al., Phys. Lett. B **664**, 52 (2008), ISSN 0370-2693, URL http://www.sciencedirect.com/science/article/pii/S0370269308005182.

[3] M. Karny et al., Phys. Rev. Lett. **90**, 012502 (2003).

[4] R. Grzywacz, M. Karny, K. P. Rykaczewski, J. C. Batchelder, C. R. Bingham, D. Fong, C. J. Gross, W. Krolas, C. Mazzocchi, A. Piechaczek, et al., Eur. Phys. J. A **25**, 145 (2005), URL https://doi.org/10.1140/epjad/i2005-06-210-2.

[5] T. N. Ginter, J. C. Batchelder, C. R. Bingham, C. J. Gross, R. Grzywacz, J. H. Hamilton, Z. Janas, M. Karny, A. Piechaczek, A. V. Ramayya, et al., Phys. Rev. C **68**, 034330 (2003), URL https://link.aps.org/doi/10.1103/PhysRevC.68.034330.

[6] J. C. Batchelder, M. Tantawy, C. R. Bingham, M. Danchev, D. J. Fong, T. N. Ginter, C. J. Gross, R. Grzywacz, K. Hagino, J. H. Hamilton, et al., Eur. Phys. J. A **25**, 149 (2005), URL https://doi.org/10.1140/epjad/i2005-06-010-8.

[7] E. Maglione and L. S. Ferreira, Phys. Rev. C **61**, 047307 (2000), URL https://link.aps.org/doi/10.1103/PhysRevC.61.047307.

[8] P. Arumugam, L. S. Ferreira, and E. Maglione, Phys. Rev. C **78**, 041305(R) (2008), URL https://link.aps.org/doi/10.1103/PhysRevC.78.041305.

[9] P. Arumugam, L. Ferreira, and E. Maglione, Phys. Lett. B **680**, 443 (2009), ISSN 0370-2693, URL http://www.sciencedirect.com/science/article/pii/S0370269309011071.

[10] C. J. Gallagher, Jr. and S. A. Moszkowski, Phys. Rev. **111**, 1282 (1958).

[11] N. D. Newby, Phys. Rev. **125**, 2063 (1962).

[12] P. Siwach, P. Arumugam, S. Modi, L. S. Ferreira, and E. Maglione, Phys. Rev. C **103**, L031303 (2021), URL https://link.aps.org/doi/10.1103/PhysRevC.103.L031303.

[13] K. Hagino, Phys. Rev. C **64**, 041304(R) (2001), URL https://link.aps.org/doi/10.1103/PhysRevC.64.041304.

[14] J. M. Yao, B. Sun, P. J. Woods, and J. Meng, Phys. Rev. C **77**, 024315 (2008), URL https://link.aps.org/doi/10.1103/PhysRevC.77.024315.

[15] S. Modi, M. Patial, P. Arumugam, L. S. Ferreira, and E. Maglione, Phys. Rev. C **96**, 064308 (2017), URL https://link.aps.org/doi/10.1103/PhysRevC.96.064308.

[16] G. Fiorin, E. Maglione, and L. S. Ferreira, Phys. Rev. C **67**, 054302 (2003), URL https://link.aps.org/doi/10.1103/PhysRevC.67.054302.

[17] J. C. Batchelder, M. Tantawy, C. R. Bingham, M. Danchev, D. J. Fong, T. N. Ginter, C. J. Gross, R. Grzywacz, K. Hagino, J. H. Hamilton, et al., in *The 4th International Conference on Exotic Nuclei and Atomic Masses*, edited by C. J. Gross, W. Nazarewicz, and K. P. Rykaczewski (Springer Berlin Heidelberg, Berlin, Heidelberg, 2005), pp. 149–150, ISBN 978-3-540-37642-2.

[18] P. Siwach, P. Arumugam, S. Modi, L. S. Ferreira, and E. Maglione, J. Phys. G: Nucl. Part. Phys. **47**, 125105 (2020), URL https://doi.org/10.1088%2F1361-6471%2Fabb6c2.

[19] P. Siwach, P. Arumugam, L. Ferreira, and E. Maglione, Phys. Lett. B **811**, 135937 (2020), URL http://www.sciencedirect.com/science/article/pii/S0370269320307401.

[20] E. Maglione, L. S. Ferreira, and R. J. Liotta, Phys. Rev. Lett. **81**, 538 (1998), URL https://link.aps.org/doi/10.1103/PhysRevLett.81.538.

[21] P. Moller, R. Bengtsson, B. Carlsson, P. Olivius, T. Ichikawa, H. Sagawa, and A. Iwamoto, At. Data Nucl. Data Tables **94**, 758 (2008).

[22] B. Blank and M. J. G. Borge, Prog. Part. and Nucl. Phys. **60**, 403 (2008).

[23] M. N. Tantawy, C. R. Bingham, K. P. Rykaczewski, J. C. Batchelder, W. Królas, M. Danchev, D. Fong, T. N. Ginter, C. J. Gross, R. Grzywacz, et al., Phys. Rev. C **73**, 024316 (2006), URL https://link.aps.org/doi/10.1103/PhysRevC.73.024316.

[24] S. V. Lukyanov, E. Maglione, and L. S. Ferreira (AIP, 2003), vol. 681, p. 77.

[25] G. Audi, O. Bersillon, J. Blachot, and A. Wapstra, Nucl. Phys. A **729**, 3 (2003), ISSN 0375-9474, the 2003 NUBASE and Atomic Mass Evaluations, URL http://www.sciencedirect.com/science/article/pii/S0375947403018074.

[26] A. Bohr and B. R. Mottelson, *Nuclear Structure*, vol. II (Benjamin, New York, 1969).

[27] D. Seweryniak et al., Phys. Rev. Lett. **99**, 082502 (2007).

[28] D. Seweryniak, P. J. Woods, J. J. Ressler, C. N. Davids, A. Heinz, A. A.Sonzogni, J. Uusitalo, W. B. Walters, J. A. Caggiano, M. P. Carpenter, et al., Phys. Rev. Lett. **86**, 1458 (2001).

[29] D. T. Doherty, A. N. Andreyev, D. Seweryniak, P. J. Woods, M. P. Carpenter, K. Auranen, A. D. Ayangeakaa, B. B. Back, S. Bottoni, L. Canete, J. G. Cubiss, J. Harker, T. Haylett, T. Huang, R. V. F. Janssens, D. G. Jenkins, F. G. Kondev, T. Lauritsen, C. Lederer-Woods, J. Li, C. Müller-Gatermann, D. Potterveld, W. Reviol, G. Savard, S. Stolze, S. Zhu, Solving the puzzles of the decay of the heaviest known proton-emitting nucleus ^{185}Bi, Phys. Rev. Lett. 127 (2021) 202501. doi:10.1103/PhysRevLett.127.202501. URL https://link.aps.org/doi/10.1103/PhysRevLett.127.202501